



Temperature-tunable UV generation using an Alexandrite laser and PPLN waveguides

GORONWY TAWY,^{1,*}  NOELIA PALOMAR DAVIDSON,¹ GLENN CHURCHILL,¹ MICHAEL J. DAMZEN,² PETER G. R. SMITH,¹  JAMES C. GATES,¹ AND CORIN B. E. GAWITH^{1,3} 

¹*Optoelectronics Research Centre, University of Southampton, Southampton, Hampshire SO17 1BJ, UK*

²*Photonics Group, Department of Physics, Imperial College London, London SW7 2AZ, UK*

³*Covesion Ltd., Unit F3, Adanac North, Adanac Drive, Nursling, Southampton SO16 0BT, UK*

**g.l.tawy@soton.ac.uk*

Abstract: We present a simple and novel technique for achieving ultra-violet (UV) wavelength-tunable laser operation in the continuous-wave regime. Wavelength tunable operation in the near infrared is obtained from a compact two-mirror Alexandrite laser cavity by temperature tuning of the laser crystal. Second-harmonic-generation to the UV is then achieved at 376-379 nm and 384-386 nm by temperature tuning of a periodically-poled lithium-niobate (PPLN) waveguide. A maximum UV power of 1.3 mW from 185 mW infra-red pump throughput is obtained from a third-order PPLN $\Lambda = 6.1 \mu\text{m}$ grating. These results show promising potential for simple and wavelength tunable access to wavelengths at 360-400 nm.

Published by Optica Publishing Group under the terms of the [Creative Commons Attribution 4.0 License](https://creativecommons.org/licenses/by/4.0/). Further distribution of this work must maintain attribution to the author(s) and the published article's title, journal citation, and DOI.

1. Introduction

Compact and low-cost laser devices emitting in the ultra-violet (UV) are of growing importance in quantum technologies such as atom cooling [1] and quantum computing [2]. 375 nm single transverse mode diodes with ~ 70 mW output power are commercially available but have limited wavelength versatility and power-scaling. Frequency-converted $1 \mu\text{m}$ and $1.5 \mu\text{m}$ lasers have better brightness but limited tunability and require multiple conversion stages to reach the UV. Frequency doubled Ti:Sapphire lasers provide single-step access but typically require diode-pumped solid-state laser pumping making them bulky and expensive. Alternatively, frequency conversion from other tunable near-infrared (700-800 nm) lasers such as Alexandrite (Cr:BeAl₂O₄) [3] and Cr:LiSAF [4] provides direct single-step access to the UVA range with the ease and compactness of direct diode-pumping. Alexandrite lasers are particularly promising as they offer low threshold [5], high efficiency, power handling [6] and high-energy storage [7]. The ability of Alexandrite lasers to operate efficiently across a broad temperature range is a further unique advantage [5,8].

Quasi-phase matching via periodically-poled non-linear optical materials has become the preferential choice for frequency conversion owing to the lack of walk-off as well as wavelength and polarisation flexibility. Periodically-poled lithium niobate (PPLN) is one of the most popular materials in the visible and UVA-band due to its high damage threshold and high non-linearity [9]. Recent progress in PPLN waveguides has realized high 70 % efficiency Watt-level second-harmonic generation (SHG) from continuous-wave (CW) laser sources in the near-infrared [10,11]. Zinc doped and indiffused MgO-doped PPLN waveguides have been shown as an effective method of reaching the UV with low absorption [12,13].

Our aim is to use the advantages of both diode-pumped Alexandrite lasers and PPLN waveguides for a simple wavelength versatile source in the UV. We present a temperature tunable

Alexandrite laser operating at 752-758 nm and 788-793 nm over 50-200 °C. Diffraction limited output ($M^2 < 1.1$) with up to 0.88 W from a compact setup is obtained. SHG provides 376-379 nm and 384-386 nm tunable UV output using PPLN waveguides. 1.3 mW at 185 mW throughput pump power is obtained at 378.3 nm - a normalized conversion efficiency of $3.65\% \text{ W}^{-1}$. This result represents the first demonstration of a fully temperature tuned UV source via SHG of a diode-pumped Alexandrite laser with potential to access anywhere within 360-400 nm.

2. Temperature tunable Alexandrite laser

Figure 1 shows a schematic diagram of our Alexandrite laser. The Alexandrite crystal used in this work is from Crystech with a nominal Cr-doping of 0.2 at.% and is Brewster-cut with dimensions of $4 \times 4 \times 5 \text{ mm}^3$. The absorption coefficients measured at 633 nm are $\alpha_a = 0.3 \text{ cm}^{-1}$ and $\alpha_b = 6.2 \text{ cm}^{-1}$ along the a and b axes, respectively.

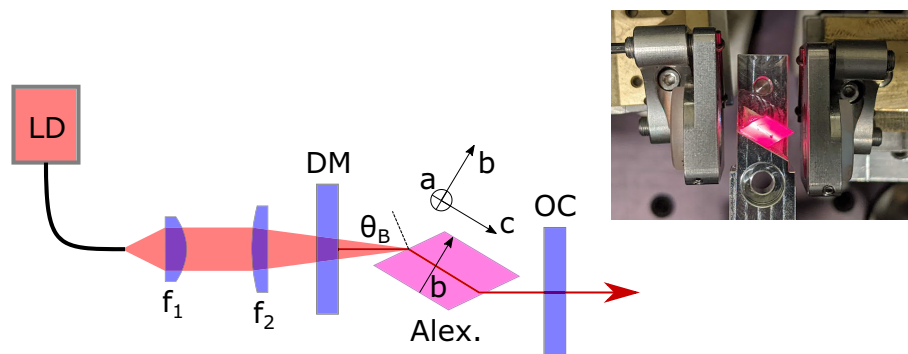


Fig. 1. Schematic diagram of a laser diode pumped Alexandrite laser cavity. Inset: photograph of laser cavity.

A dichroic mirror (DM) and output coupler (OC) with $R_{OC} = 99\%$ are used to form a plane-plane cavity with a cavity length of $< 20 \text{ mm}$. A $105 \mu\text{m}$ core diameter fiber-coupled red diode is used as the pump source with 4 W of linearly polarized output power at 635 nm. A pump waist size of $w_p = 120 \mu\text{m}$ (using a $f_1 = 11 \text{ mm}$ and $f_2 = 25 \text{ mm}$ telescope) was used with a Rayleigh length of $z_R = 1.4 \text{ mm}$. The Alexandrite crystal is mounted onto a peltier oven ($\pm 0.01^\circ\text{C}$ stability). At maximum pump power this enables the temperature of the crystal to be varied from 50-200 °C.

Figure 2 shows the laser power as a function of the absorbed pump power. A maximum output laser power of 0.88 W at 757 nm from the Alexandrite laser was measured for 3.8 W of absorbed pump power, with a slope efficiency of 41%. The output mode was slightly elliptical due to the Brewster-cut but was diffraction limited with a measured beam quality of $M^2 < 1.1$ in both directions. A capture of the beam in the far-field is included in Fig. 2 as well as the laser spectrum at 55 °C, which was centred at 757.0 nm with a FWHM of 0.2 nm (0.02 nm optical spectrum analyser resolution).

The wavelength of a laser containing a Brewster-cut birefringent gain medium without any other wavelength selective component is given by $\lambda = \Delta n L / m$, where Δn is the refractive index difference ($\Delta n \approx n_b - n_a = 0.0055$ for light along the c -axis [14]), $L = 5 \text{ mm}$ is the crystal length and m is an integer. The crystal acts as a birefringent filter, and wavelength tuning can therefore be achieved by change of orientation or temperature of the crystal. Further details of the properties and of the tuning effect can be found in [14]. Wavelength tuning is limited by the free spectral range of the crystal which is given by $\text{FSR} = \lambda^2 / \Delta n L \approx 20 \text{ nm}$.

Figure 3(a) shows Alexandrite laser wavelength as a function of oven temperature. At around 50-120 °C there is a gradual blue-shift in the laser wavelength. At 125 °C the laser wavelength

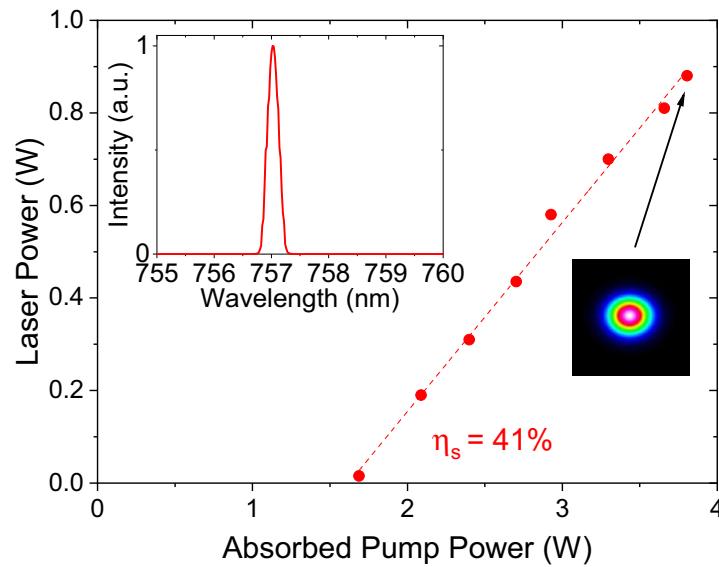


Fig. 2. Alexandrite output power as a function of absorbed laser diode pump power, with crystal operated at 50 °C. Inset: spectrum and mode profile at 0.88 W laser power.

jumps from 752 nm to 772 nm and almost immediately again to 793 nm. This can lead to dual wavelength operation as shown in Fig. 3(c) with a peak-to-peak separation of 20.6 nm - matching well to the theoretical FSR. At around 125-200 °C the laser wavelength again gradually blue-shifts.

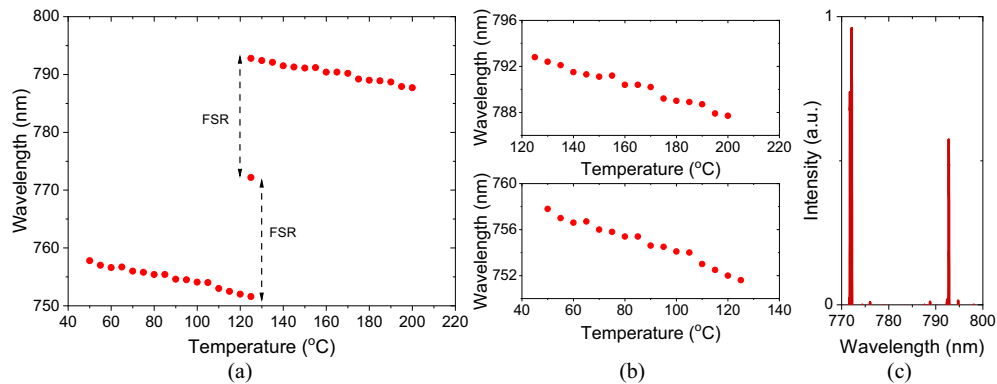


Fig. 3. Laser wavelength as a function of crystal temperature at: (a) 50-200 °C (b) selected temperature ranges. (c) Dual wavelength spectrum at 135 °C.

The laser wavelength at 200 °C is longer than that at 50 °C due to an inherent red-shift in the peak of the emission cross section with increased temperature [15]. However, at smaller increments there is a gradual blue-shift due to the temperature dependence of the refractive index components. This effect has been previously observed over a small [14] and large temperature range [5].

These results allow two wavelength tuning regions to be investigated for second-harmonic-generation: 752-758 nm and 788-793 nm. In principle, fine-tuning along any part of the tuning

band of Alexandrite (720-820 nm) can be achieved by tailoring the reflectivity of the cavity optics and/or by selecting a suitable crystal length to obtain the desired FSR.

3. UV generation

3.1. PPLN waveguide

Two PPLN waveguides are used in this experiment for enabling Type-0 SHG at the two wavelength ranges of 752-758 nm and 788-793 nm, both fabricated by the same procedure as outlined in [13]. A 0.5 mm thick 5% magnesium-doped lithium-niobate wafer is periodically poled via application of an electric field to form a poling period Λ into the wafer. For vertical confinement a metallic zinc layer is deposited and indiffused in an oxygen-rich environment. Ductile dicing is used to form the air-surrounded waveguide for horizontal confinement as well as cutting of the end-facets. Multiple waveguides of varying ridge width (nominally 4-8 μm in 0.5 μm steps) are cut into a single chip. Further details of the fabrication procedure can be found in [16]. For 788-793 nm SHG a first-order PPLN grating was used with $\Lambda = 2.2 \mu\text{m}$ and 14 mm length with 90° facets - similar to that used in [13]. For the 752-758 nm SHG range a new design is used. This has a poling period of $\Lambda = 6.1 \mu\text{m}$ for a third-order interaction and a length of 20 mm with 5.3° angle-cut to minimize back reflections. Despite the lower efficiency compared to first-order gratings, third-order poling provides the technical advantage of easier fabrication (especially compared to periods on the order of 2 μm) and therefore ensures better repeatability and scalability in manufacturing.

3.2. SHG experimental setup

Figure 4 shows the experimental setup for SHG using each PPLN waveguide. A free-space fiber-launch system is used for coupling the pump laser light into the waveguide. The laser output is coupled into a polarisation maintaining (PM) fiber via an adjustable fiber collimator (f_{ac}) with a free-space isolator included for preventing any feedback. A half-wave plate ($\lambda/2$) is used to optimize the launched polarisation. The fiber output is connected to a zoom collimator (f_{zc}) and an aspheric lens of focal length $f_l = 11 \text{ mm}$ is used to focus the pump into the waveguide - enabling optimisation of the waist size which was around 2 μm radius. The PPLN chip is mounted onto Covesion PV20 oven for temperature control at 25-200 $^\circ\text{C}$. The throughput pump and signal are collimated by a secondary aspheric lens of focal length $f_c = 11 \text{ mm}$. Both the pump launch and collimating lens are mounted on six-axis manual stages for fine control. A longpass filter (LP) is used to separate the pump and signal for simultaneous measurement of the power using two photo-diode (PD) power sensors. An additional colour filter is used to further eliminate any stray pump light when measuring the signal. A scanning-slit beam profiler is used to record the mode profile and all spectra are recorded with an optical spectrum analyser (0.02 nm resolution).

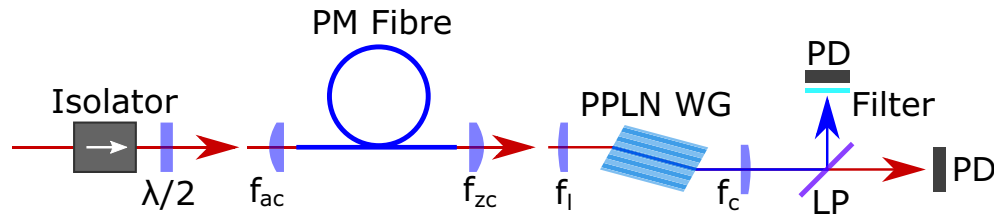


Fig. 4. SHG setup using free-space fiber coupling into angle-cut PPLN waveguide (WG).

The fiber output is connected to a zoom collimator (f_{zc}) and an aspheric lens of focal length $f_l = 11 \text{ mm}$ is used to focus the pump into the waveguide - enabling optimisation of the waist size which was around 2 μm radius. The PPLN chip is mounted onto Covesion PV20 oven for temperature control at 25-200 $^\circ\text{C}$. The throughput pump and signal are collimated by a secondary aspheric lens of focal length $f_c = 11 \text{ mm}$. Both the pump launch and collimating lens are mounted on six-axis manual stages for fine control.

A longpass filter (LP) is used to separate the pump and signal for simultaneous measurement of the power using two photo-diode (PD) power sensors. An additional colour filter is used to further eliminate any stray pump light when measuring the signal. A scanning-slit beam profiler is used to record the mode profile and all spectra are recorded with an optical spectrum analyser (0.02 nm resolution).

4. Results

Figure 5(a) shows the temperature phase matching curves for the first-order $\Lambda = 2.2 \mu\text{m}$ PPLN waveguide using 788-793 nm SHG at four wavelengths, with a higher-resolution phase matching curve at 792.9 nm shown in Fig. 5(b). Here the conversion efficiency is defined as SHG power divided by the pump throughput power to address coupling loss. Figure 6 shows the UV spectra for each phase matching experiment. The following results are for the $4 \mu\text{m}$ wide waveguide which achieved the best efficiency.

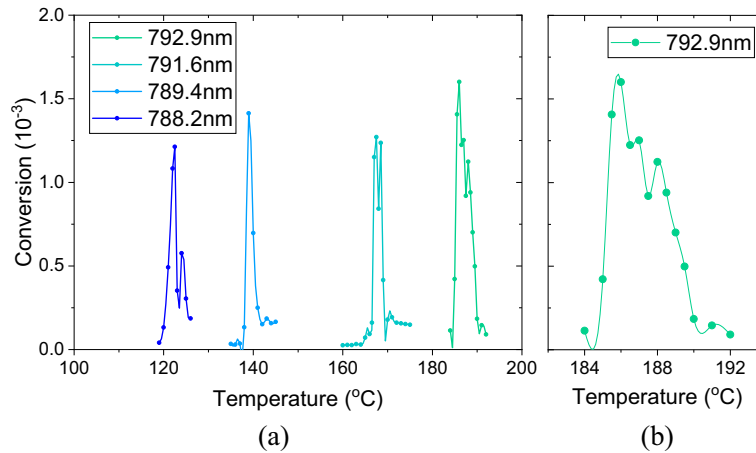


Fig. 5. 788-793 nm doubling with $\Lambda = 2.2 \mu\text{m}$ grating. (a) Conversion efficiency (signal power divided by throughput pump power) as a function of PPLN waveguide temperature at four pump wavelengths. (b) Conversion efficiency for 792.9 nm.

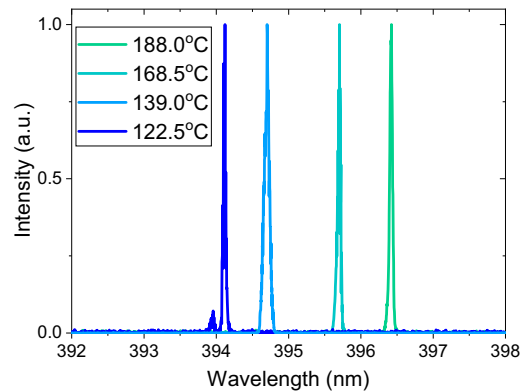


Fig. 6. Normalized UV spectra from phase matching experiments at 788-793 nm.

Tunable operation at 394.1-396.4 nm with $<0.1 \text{ nm}$ linewidth was obtained with variation of both the laser crystal temperature to set the pump wavelength and PPLN temperature to phase match. $200 \mu\text{W}$ of signal power was achieved across the tuning band for a throughput pump power of around 60 mW for the 14 mm-long first-order PPLN waveguide. This is similar to our previous results obtained for frequency doubling at 782 nm at $\sim 30^{\circ}\text{C}$ [13]. This lower efficiency compared to our other PPLN waveguides [10] was primarily attributed to the difficulty in achieving good quality $2.2 \mu\text{m}$ poling. This was the motivation for also testing third-order SHG devices in the UV range.

For the $\Lambda = 6.1 \mu\text{m}$ third-order interaction, the Alexandrite laser was tuned over 751.6–758.2 nm with 375.8–379.1 nm continuous tuning of the second-harmonic achieved. Figure 7(a) shows the phase matching curves at four pump wavelengths with the corresponding UV spectra shown in Fig. 8. Figure 7(b) shows the temperature-tuned phase matching curve for a pump wavelength of 756.6 nm with a FWHM of around 3.5°C .

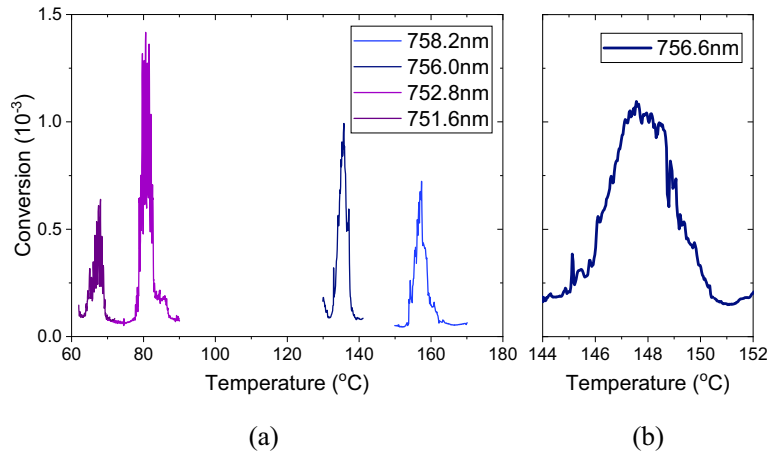


Fig. 7. 752–758 nm doubling with $\Lambda = 6.1 \mu\text{m}$ grating. (a) Conversion efficiency (signal power divided by throughput pump power) as a function of PPLN waveguide temperature at four pump wavelengths. (b) Conversion efficiency for 756.6 nm.

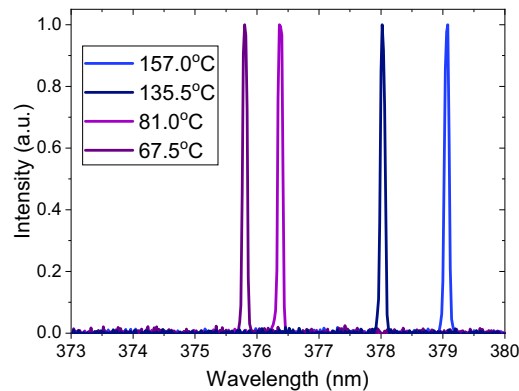


Fig. 8. Normalized UV spectra from phase matching experiments at 752–758 nm.

Figure 9 shows the signal power as a function of the throughput pump power at a pump wavelength of 756.6 nm using the third-order $\Lambda = 6.1 \mu\text{m}$ grating. Five waveguides with nominal ridge widths of 5–7 μm (with 0.5 μm increments) were tested with phase matching observed in each waveguide and the highest efficiency observed in the 7 μm wide waveguide. An image of the far-field SHG mode at the maximum measured power is also shown in Fig. 9.

A maximum signal power of 1.3 mW was obtained at a throughput pump power of 185 mW, this corresponds to a normalized conversion efficiency of $3.65\% \text{W}^{-1}$ ($1.8\% \text{W}^{-1} \text{cm}^{-2}$). The total insertion loss at the pump wavelength was approximated by comparing the incident and transmitted pump power (non-depleted) and came to around 4.5 dB or 2.3dB cm^{-1} , which includes coupling loss and the loss due to the Fresnel reflection at both facets of the uncoated

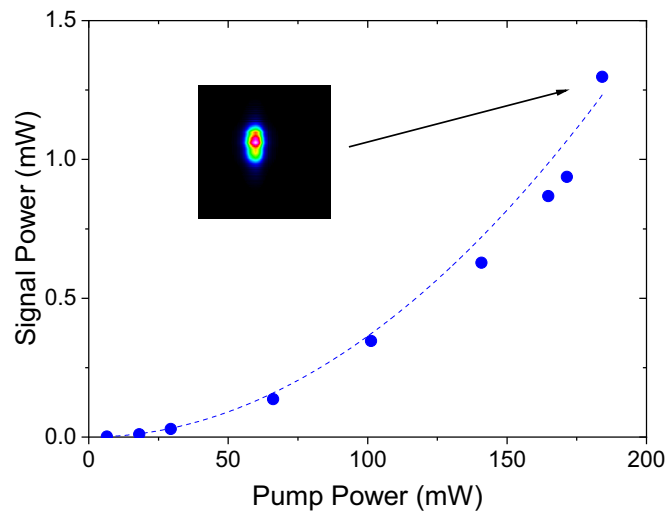


Fig. 9. Signal power at 378.3 nm as a function of the throughput pump power. Dashed line shows quadratic fitting. Inset: far-field beam profile.

waveguide. The absorption coefficient was measured using laser diodes at 785 nm and 405 nm and found to be $\alpha = 0.3 \text{ dB cm}^{-1}$ and $\alpha = 0.5 \text{ dB cm}^{-1}$, respectively.

The measured efficiency is impacted by the spectral width of the Alexandrite pump laser which was around 0.2 nm, compared to the theoretical spectral acceptance bandwidth of the PPLN crystal of around 0.1 nm. This is further evident when comparing the experimental temperature tuning bandwidth of 3.5 °C to the theoretical value of 1.8 °C [17]. The peak of the UV emission shifted by around 0.3 nm across the phase matching peak with the maximum power at 378.3 nm. In principle, a normalized conversion efficiency of $\sim 7\% \text{ W}^{-1}$ should be possible using a $<0.1 \text{ nm}$ linewidth pump source with the same waveguide.

We obtained an overall efficiency of around 0.04 % for 3.5 W of red-diode to 1.3 mW UV with losses attributed to the isolator ($\sim 5\%$), fiber-coupling ($\sim 20\%$) and waveguide insertion losses ($\sim 30\%$). While better efficiencies can be obtained from intra-cavity SHG lasers (e.g. Song et al. achieved 7.9 % [3]), high power laser diodes are required - the laser threshold was $>5 \text{ W}$. Using PPLN waveguides relaxes the multi-watt pump power requirement, and a fully packaged system (negating isolator and fiber-coupling) and improved waveguide coupling (via AR-coating and optimized launch optics) can drastically improve the efficiency with our fully temperature tunable system providing greater wavelength versatility and compactness compared to typically fixed wavelength BBO/LBO intra-cavity SHG lasers. Low-threshold and high efficiency operation of Alexandrite lasers (e.g., Yorulmaz et al. achieved a threshold of 13 mW [5]) using free-space laser diodes is another possible optimisation.

Comparing other recent work using waveguides in this wavelength range, Eigner et al. using a Ti:Sapphire pump laser and PPKTP waveguides achieved $6.6\% \text{ W}^{-1} \text{ cm}^{-2}$ normalized conversion efficiency at a signal wavelength of 396.1 nm but with only $4.9 \mu\text{W}$ signal power [18]. The same group also reported up to $88 \mu\text{W}$ (195 mW incident pump power) at 400.65 nm [19].

Our approach using a diode-pumped Alexandrite laser provides potential to access deeper UV wavelengths including 369 nm for Yb-traps in a compact (few cm^3) footprint. PPLN waveguides with third-order UV SHG offer simpler fabrication than first-order devices and with efficiencies that are appropriate for mW-level quantum technology ion trap applications.

5. Conclusion and outlook

In this work we have demonstrated the first UV tunable laser operation from a diode-pumped Alexandrite laser. Tuning ranges of 376–379 nm and 384–386 nm were obtained via SHG of a temperature-tunable Alexandrite laser using temperature tuned PPLN waveguides. A maximum SHG signal power of 1.3 mW was obtained at a throughput pump power of 185 mW. These results demonstrate the potential of this system to access any wavelength at 360–400 nm with only temperature control. The low-threshold of Alexandrite offers the potential for compact (cm³ scale) packaged devices.

In future we will present results demonstrating wider wavelength coverage as well as higher power operation. A more in-depth study of the waveguide mode structure at the fundamental and signal will also be investigated as a route to improving coupling loss. We also envisage applying the system to Yb-cooling devices at 369 nm - well within the SHG of Alexandrite. Future work will also be aimed at demonstrating pulsed operation via Q-switching.

Funding. Royal Academy of Engineering (RCSRF1718639); Engineering and Physical Sciences Research Council (EP/P027644/1, EP/T00097X/1); Innovate UK (10001664, 50414).

Disclosures. PGRS and CBEG: Covision Ltd. (E,P). All other authors declare no conflicts of interest.

Data availability. All data supporting this study are openly available from the University of Southampton repository [20].

References

1. S. Mulholland, H. A. Klein, G. P. Barwood, S. Donnellan, P. B. R. Nisbet-Jones, G. Huang, G. Walsh, P. E. G. Baird, and P. Gill, "Compact laser system for a laser-cooled ytterbium ion microwave frequency standard," *Rev. Sci. Instrum.* **90**(3), 033105 (2019).
2. A. Anwar, C. Perumangatt, F. Steinlechner, T. Jennewein, and A. Ling, "Entangled photon-pair sources based on three-wave mixing in bulk crystals," *Rev. Sci. Instrum.* **92**(4), 041101 (2021).
3. Y. Song, Z.-M. Wang, Y. Bo, F.-F. Zhang, Y.-X. Zhang, N. Zong, and Q.-J. Peng, "2.55W continuous-wave 378nm laser by intracavity frequency doubling of a diode-pumped Alexandrite laser," *Appl. Opt.* **60**(20), 5900–5905 (2021).
4. U. Demirbas and I. Baali, "Power and efficiency scaling of diode pumped Cr:LiSAF lasers: 770–1110 nm tuning range and frequency doubling to 387–463 nm," *Opt. Lett.* **40**(20), 4615–4618 (2015).
5. I. Yorulmaz, E. Beyatli, A. Kurt, A. Sennaroglu, and U. Demirbas, "Efficient and low-threshold Alexandrite laser pumped by a single-mode diode," *Opt. Mater. Express* **4**(4), 776–789 (2014).
6. G. Tawy, A. Minassian, and M. J. Damzen, "High-power 7.4W TEM₀₀ and wavelength-tunable alexandrite laser with a novel cavity design and efficient fibre-coupled diode-pumping," *OSA Continuum* **3**(6), 1638–1649 (2020).
7. S. Unland, R. Kalmes, P. Wessels, D. Kracht, and J. Neumann, "High-performance cavity-dumped Q-switched Alexandrite laser CW diode-pumped in double-pass configuration," *Opt. Express* **31**(2), 1112–1124 (2023).
8. M. Fibrich, J. Šulc, D. Vyhřídál, H. Jelínková, and M. Cech, "Alexandrite spectroscopic and laser characteristic investigation within a 78–400 K temperature range," *Laser Phys.* **27**(11), 115801 (2017).
9. D. S. Hum and M. M. Fejer, "Quasi-phase-matching," *C. R. Phys.* **8**(2), 180–198 (2007). Recent advances in crystal optics.
10. L. G. Carpenter, S. A. Berry, A. C. Gray, J. C. Gates, P. G. R. Smith, and C. B. E. Gawith, "CW demonstration of SHG spectral narrowing in a PPLN waveguide generating 2.5 W at 780 nm," *Opt. Express* **28**(15), 21382–21390 (2020).
11. S. Suntsov, C. E. Rüter, D. Brüske, and D. Kip, "Watt-level 775 nm SHG with 70% conversion efficiency and 97% pump depletion in annealed/reverse proton exchanged diced PPLN ridge waveguides," *Opt. Express* **29**(8), 11386–11393 (2021).
12. K. Mizuuchi, T. Sugita, K. Yamamoto, T. Kawaguchi, T. Yoshino, and M. Imaeda, "Efficient 340-nm light generation by a ridge-type waveguide in a first-order periodically poled MgO:LiNbO₃," *Opt. Lett.* **28**(15), 1344–1346 (2003).
13. A. C. Gray, J. R. C. Woods, L. G. Carpenter, H. Kahle, S. A. Berry, A. C. Tropper, M. Guina, V. Apostolopoulos, P. G. R. Smith, and C. B. E. Gawith, "Zinc-indiffused MgO:PPLN waveguides for blue/uv generation via VECSEL pumping," *Appl. Opt.* **59**(16), 4921–4926 (2020).
14. G. Tawy and M. J. Damzen, "Tunable, dual wavelength and self-Q-switched alexandrite laser using crystal birefringence control," *Opt. Express* **27**(13), 17507–17520 (2019).
15. M. Shand and H. Jenssen, "Temperature dependence of the excited-state absorption of alexandrite," *IEEE J. Quantum Electron.* **19**(3), 480–484 (1983).
16. L. G. Carpenter, S. A. Berry, R. H. S. Bannerman, A. C. Gray, and C. B. E. Gawith, "ZnO indiffused MgO:PPLN ridge waveguides," *Opt. Express* **27**(17), 24538–24544 (2019).
17. W. P. Risk, T. R. Gosnell, and A. V. Nurmikko, *Compact Blue-Green Lasers* (Cambridge University, 2003).

18. C. Eigner, M. Santandrea, L. Padberg, M. F. Volk, C. E. Rüter, H. Herrmann, D. Kip, and C. Silberhorn, "Periodically poled ridge waveguides in KTP for second harmonic generation in the UV regime," *Opt. Express* **26**(22), 28827–28833 (2018).
19. C. Eigner, L. Padberg, M. Santandrea, H. Herrmann, B. Brecht, and C. Silberhorn, "Spatially single mode photon pair source at 800 nm in periodically poled Rubidium exchanged KTP waveguides," *Opt. Express* **28**(22), 32925–32935 (2020).
20. G. Tawy, N. Palomar Davidson, G. Churchill, M. J. Damzen, P. G. R. Smith, J. C. Gates, and C. B. E. Gawith, "Dataset for Temperature-tunable UV generation using an Alexandrite laser and PPLN waveguides," University of Southampton (2022), <https://doi.org/10.5258/SOTON/D2678>.